FULL PAPER

Diverse Organic Field-Effect Transistor Sensor Responses from Two Functionalized Naphthalenetetracarboxylic Diimides and Copper Phthalocyanine Semiconductors Distinguishable Over a Wide Analyte Range

Weiguo Huang, Jasmine Sinha, Ming-Ling Yeh, Josué F. Martínez Hardigree, Rachel LeCover, Kalpana Besar, Ana María Rule, Patrick N. Breysse, and Howard E. Katz*

Naphthalenetetracarboxylic diimide derivatives (octyl "8" NTCDI, dimethyl-aminopropyl "DMP" NTCDI) and copper phthalocyanine (CuPc) are used to form a diverse organic field-effect transistor (OFET) sensor array. CuPc and 8-NTCDI are p-channel and n-channel semiconductors, respectively, showing expected and opposing responses to analytes. DMP-NTCDI, on the other hand, because of its ionizable side chain, shows response directions and magnitudes that are not correlated to those of the other two. The result is a distinct response pattern and unambiguous recognition ability for individual analytes. The differences are even more dramatic if the time evolution of the responses is considered. The three-response patterns obtained from representative polar, nonpolar, acidic, and basic vapors are all different, showing the potential for this approach in rapid, low-cost electronic detection of volatile compounds.

1. Introduction

Organic field-effect transistor (OFET) sensors have shown responses to numerous analytes in investigations over the last decade.[1] The scope of the analytes can be divided into several categories: gases that affect the public environment and health, such as NH_3, H_2S, NO_2, O_3 and ethylene;[2] explosive solids that concern homeland security, such as trinitrotoluene (TNT) and dinitrotoluene (DNT);[3] and biomarkers in physiological solutions that indicate a person's medical status, such as proteins and glucose.[4] Despite the progress in using OFETs to detect

such analytes, it is still a challenge to discriminate among analytes that give the same kinds of OFET responses; this challenge is especially relevant in the vapor detection field. Generally, electron-donating analyte vapors will decrease the drain current of p-channel transistors and increase the drain current of n-channel transistors on exposure. For electron-withdrawing analyte vapors, the effect on transistors is the opposite. Therefore, typical OFETs can only discriminate between electron-donating vapors and electron-withdrawing vapors, and it is still a challenge to discriminate vapors within a set of exclusively electron-donating or electron-withdrawing species. Several groups have attempted to improve the ability of OFETs to distinguish different analyte vapors.[5–12] For example, Subramanian et al also used polythiophene with different film thicknesses and alkyl chain lengths to discriminate different amine vapors.[5] Lambeth et al. developed an array of polythiophene derivatives to discriminate different volatile organic solvents,[6] such as ethanol, methylene chloride, toluene and cyclohexane. Swager et al. developed diverse chemiresistors based on covalently modified multi-walled carbon nanotubes to create sensors capable of identifying volatile organic compounds.[7] Mulchandani et al. designed porphyrin-functionalized single-walled carbon nanotube chemiresistive sensor arrays for volatile organic compounds.[9]

There are only a few examples of small molecules as sensing layers. Baldo et al. reported combinatorial detection of volatile organic compounds using metal-phthalocyanine field effect transistors;[10] however, most of the sensor arrays discriminate analytes only by the differences of response magnitude. For some other sensor arrays, large numbers of different semiconductors (or different polymer derivatives) were needed to distinguish different analytes by the differences of both response magnitude and direction.[6] Herein, we report a versatile OFET sensor array based on naphthalenetetracarboxylic diimide derivatives and copper phthalocyanine which could unambiguously discriminate analytes not only by the differences of response magnitude but also the differences of response direction. Although only three semiconductors were used, this array can

Dr. W. G. Huang, Dr. J. Sinha, M.-L. Yeh,
J. F. M. Hardigree, R. LeCover, K. Besar, Prof. H. E. Katz
Departments of Materials Science and
Engineering and of Chemistry
Johns Hopkins University
3400 North Charles Street, Baltimore, MD 21218, USA
E-mail: hekatz@jhu.edu
Prof. A. M. Rule, Prof. P. N. Breysse
Department of Environmental Health Sciences
Bloomberg School of Public Health, Johns Hopkins University
615 North Wolfe Street, Baltimore, MD 21205, USA

Materials
Views
www.MaterialsViews.com

ADVANCED
FUNCTIONAL
MATERIALS
www.afm-journal.de

FULL PAPER

distinguish as many as eight different representative analytes. To the best of our knowledge, for the amount of chemical selectivity for the number of sensing elements, this is one of the most efficient OFET sensor arrays yet reported based on small molecules as sensing layers.
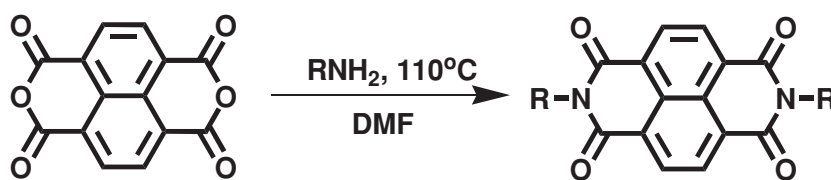
2. Results and Discussion

The chemical structures of the three semiconductors are shown in **Scheme 1**, and their corresponding transistor electrical properties are summarized in **Table 1**. DMP-NTCDI shows three orders of magnitude lower mobility compared to 8-NTCDI due to its inferior crystallinity in the film and possible charge carrier trapping by protonated amine groups in the transistor channel.[14] As shown in **Figure 1** and **2**, several orders of layer diffraction and much larger crystal grain size were observed for 8-NTCDI films, indicating its high crystallinity in thin film phase. While for DMP-NTCDI, only one peak was observed in X-ray diffraction (XRD) spectra, furthermore, small size crystal grains and numerous grain boundaries were observed in atomic force microscopy (AFM) images, indicating its inferior crystallinity in thin film phase.

We selected IPAm (isopropylamine), acetone, acetic acid, DMMP (dimethyl methylphosphate), hydrogen peroxide, water, hexane and toluene as analytes as they are common volatile compounds that have already been

$R= C_8H_{17}NH_2$ or $(CH_3)_2NCH_2CH_2CH_2NH_2$

8- NTCDI

DMP-NTCDI

CuPc

Scheme 1. Synthesis route and chemical structures of the organic semiconductors used in the sensor array.

widely considered as analytes. The drain current, mobility and threshold voltage changes of 8-NTCDI, DMP-NTCDI and CuPc over time after exposure to different analytes are shown
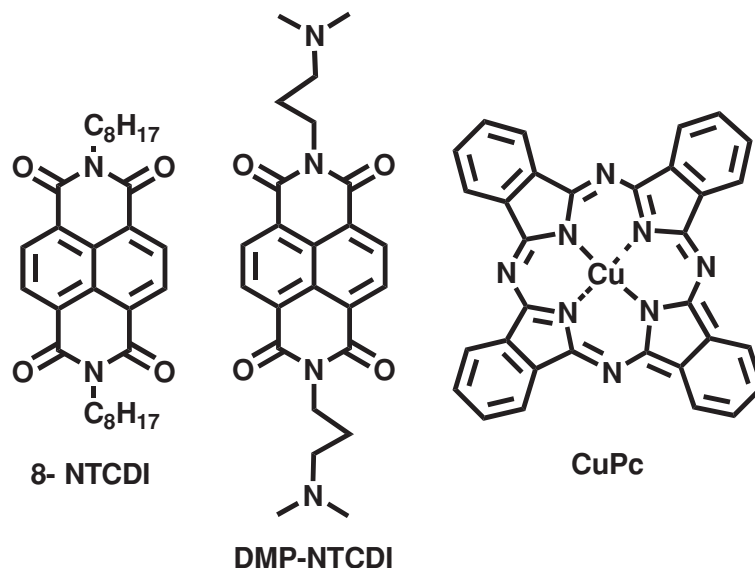
Table 1. Typical mobilities and threshold voltage changes of three OSC after exposure to the eight different analytes.

| OSCs		8- NTCDI		DMP-NTCDI		CuPc	
Analyte	Parameters	before	after	before	after	before	after
Acetic acid	μ [cm^2/V s]	9.93×10^{-3}	3.61×10^{-4}	3.17×10^{-5}	7.34×10^{-5}	4.83×10^{-3}	1.68×10^{-3}
	V_{th} [V]	42.4	63.3	6.4	−198	−18.2	−35.1
Acetone	μ [cm^2/V s]	1.85×10^{-2}	2.48×10^{-2}	3.42×10^{-5}	1.79×10^{-5}	6.06×10^{-3}	2.72×10^{-3}
	V_{th} [V]	67.3	58.8	−18	−38	−13.8	−7.8
IPAm	μ [cm^2/V s]	3.86×10^{-2}	3.79×10^{-2}	1.98×10^{-5}	1.97×10^{-5}	5.15×10^{-3}	1.39×10^{-3}
	V_{th} [V]	64.2	32	−55.4	−77.1	−11.4	−45.9
Water	μ [cm^2/V s]	1.11×10^{-2}	5.83×10^{-3}	1.84×10^{-5}	5.58×10^{-6}	1.76×10^{-3}	1.42×10^{-3}
	V_{th} [V]	53.1	61.5	−54.6	−103	14.1	6.4
H$_2$O$_2$	μ [cm^2/V s]	2.45×10^{-2}	2.36×10^{-2}	3.1×10^{-5}	3.04×10^{-5}	5.83×10^{-3}	7.17×10^{-3}
	V_{th} [V]	64.3	66	−15.6	−13.7	−9	−10
DMMP	μ [cm^2/V s]	9.33×10^{-3}	2.48×10^{-2}	3.5×10^{-5}	3.52×10^{-5}	7.42×10^{-3}	4.62×10^{-4}
	V_{th} [V]	71.2	69.5	−57.3	−48.4	−25.6	−16
Hexane	μ [cm^2/V s]	2.36×10^{-2}	2.12×10^{-2}	1.23×10^{-5}	1.19×10^{-5}	9.34×10^{-3}	8.84×10^{-3}
	V_{th} [V]	46.7	47.8	−11.6	−16.9	−3.3	−8.8
Toluene	μ [cm^2/V s]	2.4×10^{-2}	1.5×10^{-2}	6.49×10^{-5}	1.46×10^{-4}	7.76×10^{-3}	3.4×10^{-3}
	V_{th} [V]	49.6	47.5	−67.7	−4.3	−7.7	−20.5
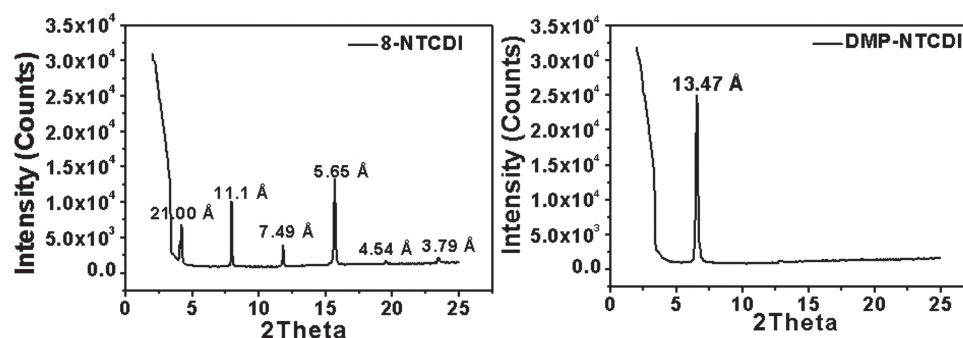
Figure 1. XRD spectra of 8-NTCDI (left) and DMP-NTCDI (right) films.

in **Figure 3**, **4** and **5**. Broadly, the sets of three plots in each of these figures are very different from each other, illustrating that the array gives an excellent qualitative discrimination among all these analytes. Trends are apparent almost immediately after exposure, except for 5-min induction periods with acetone and DMMP.

As shown in Figure 3a, the drain current of 8-NTCDI and CuPc decreased 98% and 78% after 2 min exposure to 10 μL acetic acid with the decreases saturating in 5 min, while for DMP-NTCDI, the drain current drastically increased 870% and

2200% in 2 min and 5 min, respectively, with the increase saturating in 10 min. For CuPc, the drain current decrease is attributed to the decrease of mobility and increase of threshold voltage (becoming harder to turn on). A possible reason may be that highly polar acetic acid creates more deep traps in the transistor channel, thus decreasing mobility and increasing the number of charge carriers needed to fill them before the device can be turned on. Another reason may be that acetic acid could interact with CuPc by protonation of the nitrogen atoms bridging the pyrrole rings, and ion interaction between CH_3COO^- and Cu^{2+} or
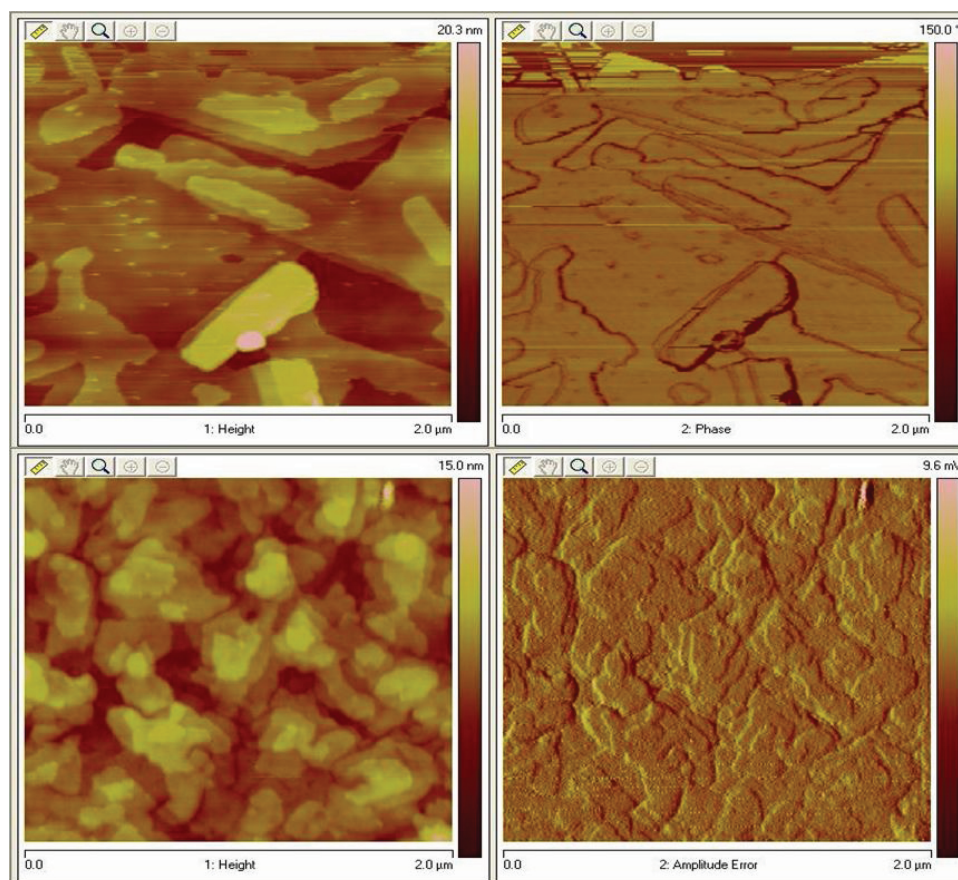
Figure 2. 2 μm × 2 μm AFM topography images of 8-NTCDI films (top) and DMP-NTCDI films (down) on HMDS treated substrates. The films were deposited at 25 °C.

www.MaterialsViews.com

ADVANCED
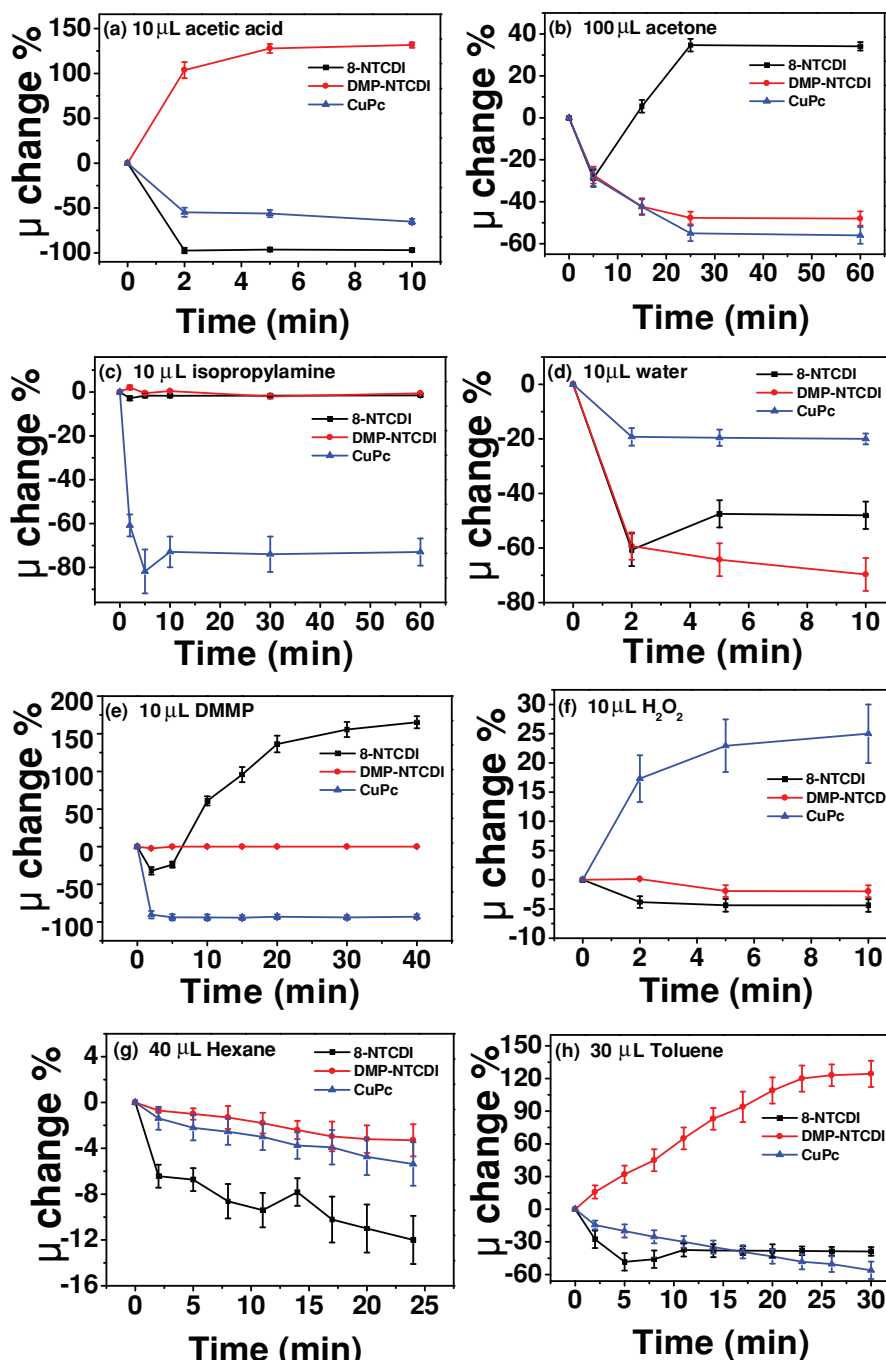FUNCTIONAL
MATERIALS
www.afm-journal.de

FULL PAPER
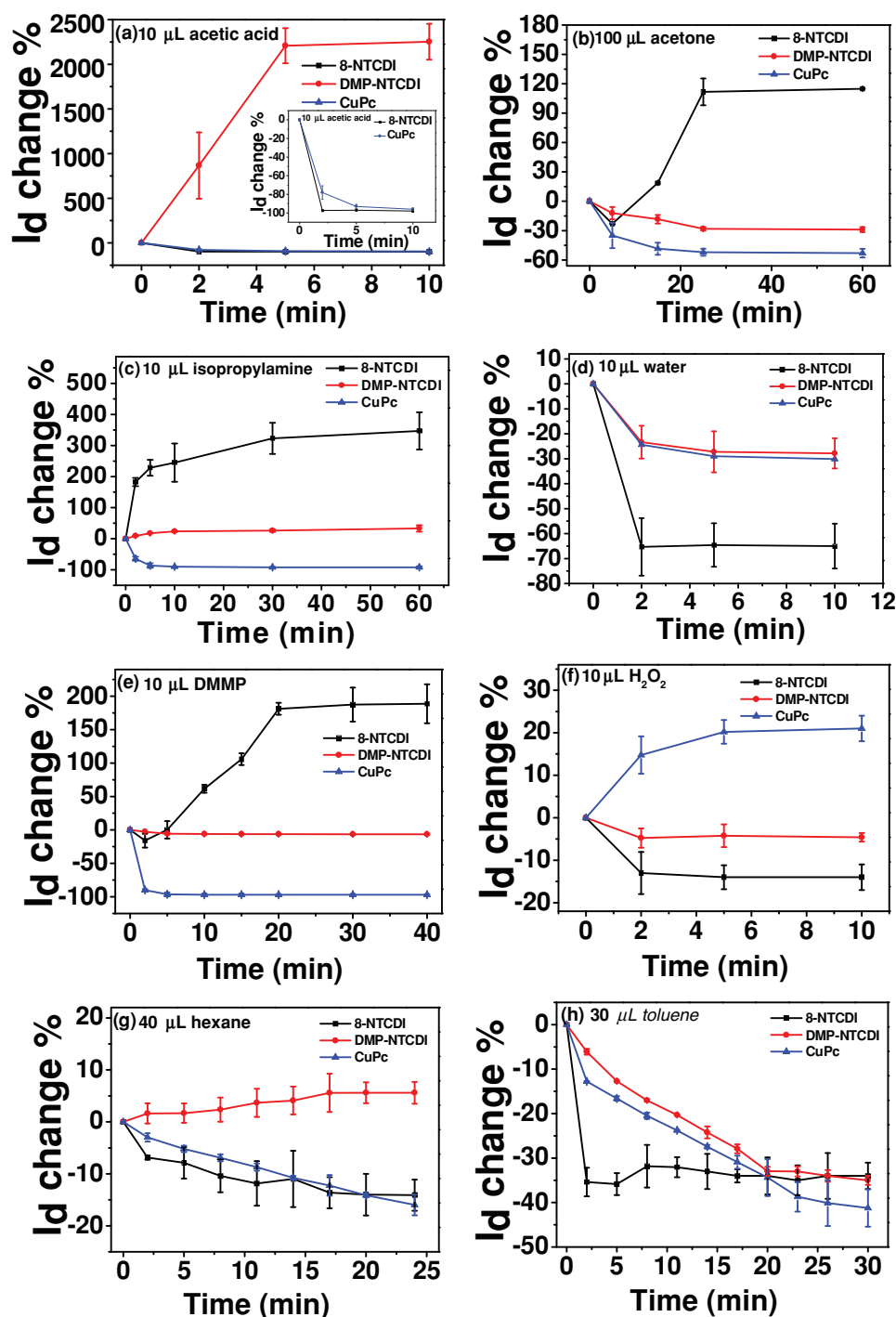
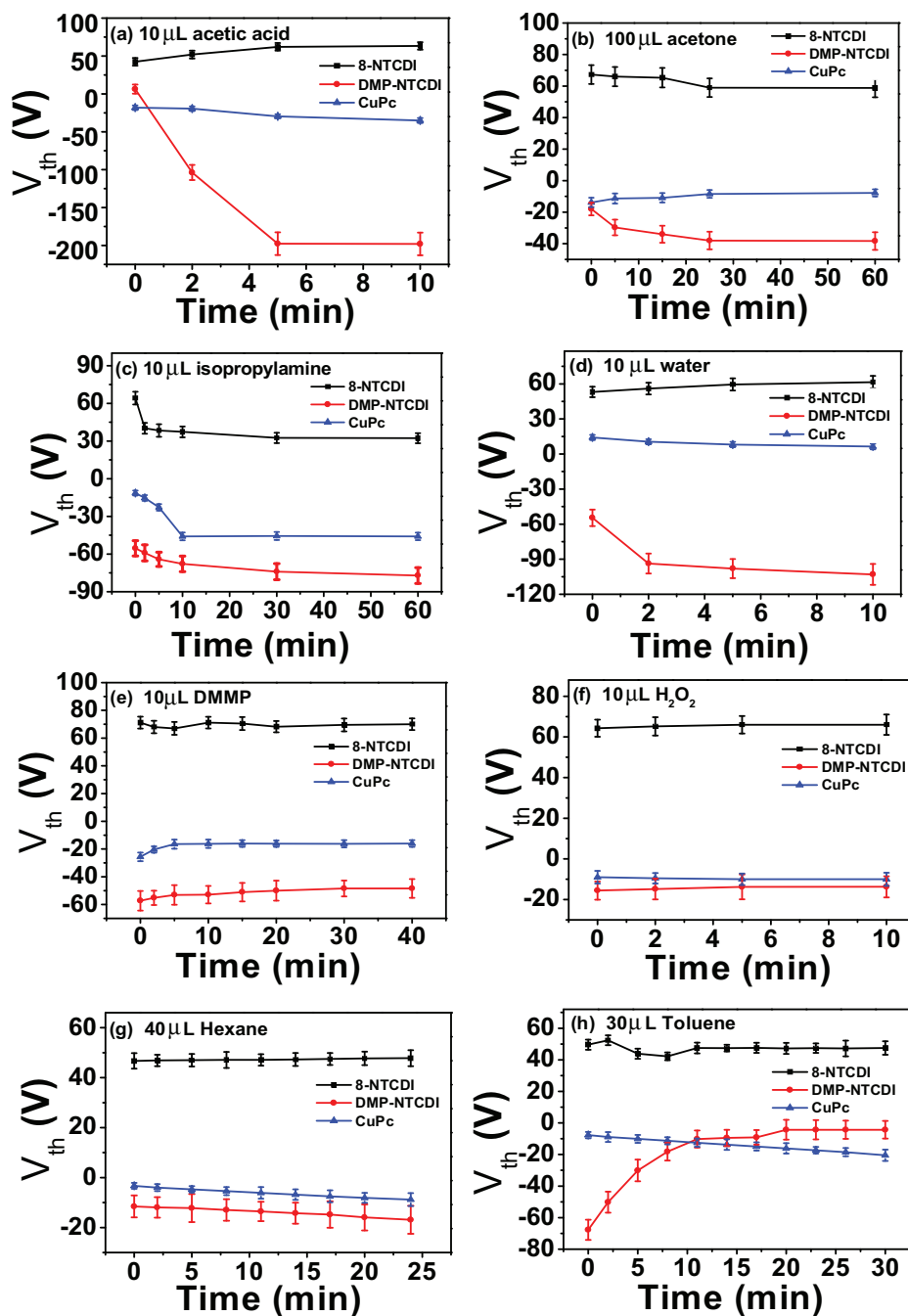**Figure 3.** Drain current change of 8-NTCDI, DMP-NTCDI and CuPc to different analytes at different time interval. The range of Y error bar in the figure indicates standard deviation.

protonated nitrogen atom NH⁺, thus generating effective impurities in the film, and decreasing the mobility[15] (see Supporting Information). For 8-NTCDI, the decrease of drain current after exposure to acetic acid is mainly due to the large (almost 30-fold) decrease of mobility. This is also because of the percolation of the highly polar acetic acid through the grain boundaries where

it interacts with charges to produce traps and increased potential barriers.[15] For DMP-NTCDI, the trapping effect still exists but it does not dominate the change of drain current. Instead, the base-acid interaction between dimethylpropyl amine groups and acetic acid, which creates numerous ion pairs in the film, drastically increases the conductivity, and thus gives a much higher

FULL PAPER

Figure 4. Mobility change of 8-NTCDI, DMP-NTCDI and CuPc to different analytes at different time intervals. The range of Y error bar in the figure indicates standard deviation.

drain current. On the other hand, the threshold voltage of the DMP-NTCDI OFET becomes much more negative, from 6.4 V to −200 V, making it much easier to turn on; this may due to the alignment of the analyte dipoles in such a way that they act as added effective gate voltage and a decrease in threshold voltage (increase in drain current) occurs.[15]

Acetone is weakly electron-donating; all three semiconductors show low sensitivities to it (Figure 3b). Although the threshold voltage of CuPc becomes slightly more positive (from

−13.8 to −7.8 V, becoming easier to turn on), the mobility of CuPc decreased more than 50% after 10 min of exposure to 0.1 mL acetone, and this mainly contributes to decreased drain current. The threshold voltages of both DMP-NTCDI and 8-NTCDI decrease after exposure to acetone due to the analyte inducing charge,[15] making these devices easier to turn on. However, the magnitude of threshold voltage change is different, probably due to their different film structures and morphologies. The short and branched structure of the

Figure 5. Threshold voltage change of 8-NTCDI, DMP-NTCDI and CuPc to different analytes at different time intervals. The range of Y error bar in the figure indicates standard deviation.

dimethylaminopropyl chain would be expected to weaken the interaction among DMP-NTCDI molecules, making the film loosely packed with more grain boundaries and allowing more acetone vapor to diffuse into the interface between the semiconductor and dielectric layer, thus giving a greater decrease of threshold voltage; while 8-NTCDI is compactly packed and with much more ordered film structure (see Figure 1 and 2), as a result, the change in threshold voltage is smaller and mobility increases. The mobility also decreased considerably for DMP-NTCDI, since a hopping mechanism dominates the conduction in such materials, the intercalation of a gas molecule between two hopping sites can increase the energy barrier by increasing the distance between hopping centers, thus causing a decrease in mobility.[14] As a result of all these factors, DMP-NTCDI only gives <30% current decrease, while for 8-NTCDI, the drain current increases about 110% after exposure to acetone, it should be noted that there is an initial current decrease (about 20%) for 8-NTCDI on exposure to acetone due to the

ADVANCED
FUNCTIONAL
MATERIALS
www.afm-journal.de

Materials Views
www.MaterialsViews.com

trapping effect, and then the current starts to increase as the effect of induced channel charge overwhelms the trapping effect.[15] Interestingly, in the recovery process, there is an initial current increase for 8-NTCDI on removal of acetone by applying vacuum (see Supporting Information). This indicates that while applying vacuum, the trapping effect is reduced faster than the effect of induced channel charge.

IPAm is strongly electron donating. For CuPc, the drain current sharply decreases after exposure to IPAm, since both mobility and threshold voltage show a large decrease.[16] For 8-NTCDI and DMP-NTCDI, the drain current increases after exposure; however, DMP-NTCDI shows a much smaller increase compared to 8-NTCDI. In both cases, the threshold voltage becomes much smaller, which makes the devices much easier to turn on. While the mobility of both semiconductors stays almost constant, the drain current changes are a consequence of the threshold voltage change, since the relative percentage change of "$V_g - V_{th}$" of 8-NTCDI is much higher than that of DMP-NTCDI. Thus, the drain current of 8-NTCDI is increased much more.

Water is a much weaker electron donor compound compared with IPAm, so this is one reason that water causes less drain current change than IPAm does. Normally water causes degradation of electronic devices; with some exceptions,[18] both n- and p-channel OFETs can decay after exposure to water. We also observe the same phenomenon; all three devices show current decrease while exposed to water due to the trapping effect[18] or degradation of interfaces between semiconductor and dielectric layers. The mobility of all three semiconductors was decreased; furthermore, 8-NTCDI and CuPc OFETs become harder to turn on, while DMP-NTCDI becomes easier to turn on.

DMMP is a weakly basic compound and simulates phosphonate nerve agents. There are multiple possible types of interactions between DMMP and semiconductor films. First, the large DMMP dipole moment (μ = 3–3.62 D), can induce strong electric fields in the immediate vicinity of the adsorbed molecules (not in the whole channel), which causes interactions with a significant fraction of the mobile charges.[1h] Second, the large molecular size of DMMP can also increase the distance of hopping centers by intercalating between two hopping sites. The mobility change of semiconductor films was seemingly dominated by these two effects. For CuPc, both effects tend to decrease mobility; thus more than 90% mobility decrease is observed in a CuPc device after exposure to DMMP. As a result, a more than 90% current decrease is observed although the threshold voltage slightly increases. For DMP-NTCDI, the first effect tends to increase the mobility of semiconductor films slightly, however, due to the loose packing of the film, the easy diffusion of DMMP into the bulk film will lead to an increase in threshold voltage (from –57 V to –48 V), thus the drain current decreases 6% for DMP-NTCDI after exposure to DMMP. For 8-NTCDI, the first effect tends to increase the mobility and it dominates the change in mobility of the film since the diffusion of large size DMMP molecules into the compact 8-NTCDI film is more difficult, while the threshold voltage stays almost constant; as a result, the drain current increased 190% for 8-NTCDI after exposure to DMMP. Also, there is an initial current decrease (about 20%) for 8-NTCDI on exposure to DMMP, and then a subsequent increase as mobility increases. Also

in the recovery process, there is an initial current increase on removal of DMMP by applying vacuum.[15]

Vapor phase monitoring of hydrogen peroxide is an important industrial health issue due to its widespread use and toxicity,[17] and is also relevant to homeland security due to the potential use of hydrogen peroxide in explosive weapon fabrication. Because of its oxidative capability (electron accepting ability),[17] hydrogen peroxide causes current gains in CuPc sensors, while for 8-NTCDI and DMP-NTCDI, the current decreases slightly after exposure to hydrogen peroxide.

As expected, this sensor array shows relatively low sensitivity to nonpolar analytes such as hexane and toluene that have small dipole moments (0.08 D for hexane, 0.36 D for toluene). For CuPc, after exposure to hexane for 25 min, the drain current decreases about 15%, with the mobility and threshold voltage slightly shifted. The drain current shows higher decrease (40%) after CuPc exposure to toluene than hexane since the dipole moment of toluene is larger than that of hexane. Toluene was the only analyte for which, after brief equilibration times, two of the response traces cross; those traces are considered to have the same qualitative response. 8-NTCDI and DMP-NTCDI are slightly soluble in the hydrocarbon solvents (saturation concentrations that we observed at 298 K: in hexane, 1.03 × 10^{-4} mol/L for DMP-NTCDI, 2.45 × 10^{-4} mol/L for 8-NTCDI; in toluene, 1.15 × 10^{-2} mol/L for DMP-NTCDI, 9.06 × 10^{-2} mol/L for 8-NTCDI), and therefore these analytes might lead to swelling of films. In that case, carrier hopping distance and barrier energy increase, leading to mobility changes.[19] Due to the polar side chain of DMP- NTCDI, the interaction between hexane and DMP-NTCDI is weaker than the interaction between hexane and 8-NTCDI, therefore, the drain current of DMP-NTCDI is almost constant after exposure to hexane for 25 min, while the drain current of 8-NTCDI decreases about 13%. Toluene is a better solvent of both semiconductors (8-NTCDI and DMP-NTCDI) than hexane, thus the drain current of both semiconductors decreases about 35% after exposure to toluene for 30 min.

We use spots with different color to represent different changes qualitatively after devices are exposed to analytes for the time periods shown in Figures 3, 4 and 5. These qualitative portrayals are shown in **Tables 2**, **3** and **4** where a blue spot represents a large value (drain current, threshold voltage and mobility) decrease, and two blue spots represent a much larger value decrease, while a light blue spot means a slight value decrease. A red spot represents a large value increase, two red spots represent a much larger value increase, and an orange spot means a slight value increase. In all three tables, each analyte has its unique spot color combination, which indicates that this sensor array could unambiguously discriminate all these analytes. From Table 2, we can see that if only CuPc were used as sensor material, we can only discriminate hydrogen peroxide from seven other analyte vapors since all those vapors cause current loss in the CuPc sensor; after incorporating 8-NTCDI into this sensor array, we could only classify the rest of the seven analyte vapors into two groups by the direction of response, the first group contains IPAm, DMMP and acetone, and the second group includes water, acetic acid, hexane and toluene. However, it would still be challenging to fully distinguish the analytes in both groups. After incorporating DMP-NTCDI, we are able to

www.MaterialsViews.com

ADVANCED
FUNCTIONAL
MATERIALS
www.afm-journal.de

FULL PAPER

Table 2. Sensor array qualitative drain current change map of different analytes. Blue spot represents large current decrease, two blue spots represent much large current decrease, while light blue spot means slight current decrease. The red spot represents a large current increase, two red spots represent a much larger current increase, and orange spot means a slight current increase.

	acid	acetone	IPAM	water	DMMP	H_2O_2	hexane	toluene
CuPc	blue, blue	light blue	blue, blue	light blue	blue, blue	orange	light blue	blue
8-NTCDI	blue, blue	orange	red	blue	red	light blue	light blue	blue
DMP-NTCDI	red, red	light blue	orange	light blue	light blue	light blue	orange	blue

completely separate all the analyte vapors from each other, in the first group, DMP-NTCDI shows current increase after exposure to IPAm and current decreases on exposure to DMMP and acetone. Although DMMP and acetone give the same direction of current change, it is very easy to discriminate them since the sensitivity of this sensor array to DMMP is much higher than to acetone.

Additionally, it should be noted that although all three analytes in the first group increase the drain current of 8-NTCDI, different mechanisms were indicated by Table 1; after exposure to acetone, both mobility and threshold voltage changes contribute to the increase of drain current; after exposure to IPAm, drain current increase is mainly attributed to the threshold voltage change as the mobility stays nearly constant; while after exposure to DMMP, the mobility change dominates the change of drain current, since no obvious shift in threshold voltage was observed. In the second group, DMP-NTCDI shows more than three orders of magnitude current increase on exposure to acetic acid and more than 20% current decrease after exposure to water and toluene. Although hexane gives the same direction of response as acetic acid, the magnitude of response is orders of magnitude different; also, water and toluene vapors both cause drain current decreases for all three semiconductors; however, the time for the three semiconductors to reach

saturated response is much less after exposure to water than toluene. Additionally, the relative responses of CuPc and DMP-NTCDI to both vapors are very different when calibrated against the response by 8-NTCDI; therefore, these four analytes in the second group are also well discriminated.

Furthermore, the changes of mobility and threshold voltage are also very unique for each analyte, and they can provide even better discrimination ability to some analytes than drain current changes. For example, acetone and DMMP, water and toluene can be much better identified by mobility and threshold voltage changes, as shown in Tables 3 and 4. In all three tables, each analyte has its distinct spot color combination. Therefore, this sensor array has excellent discrimination ability for all eight analytes.

We also have investigated the concentration dependence as well as recovery behavior of the sensors in the array array (see Supporting Information Figure S1–S3). In these figures, black arrows indicate the time point for injecting analytes, and the blue arrows indicate the time for starting to remove analytes. The responses of all three devices show excellent concentration dependence. For CuPc, while exposed to acetic acid, IPAm and DMMP, the responses are very high, and only show slight differences at different concentrations, indicating that CuPc can detect much lower concentrations of acetic acid, IPAm

Table 3. Sensor array qualitative threshold voltage change map of different analytes. Blue spot represents large threshold voltage decrease; two blue spots represent much large threshold voltage decrease, while light blue spot means slight threshold voltage decrease. The red spot represents a large threshold voltage increase, two red spots represent a much larger threshold voltage increase, and orange spot means a slight threshold voltage increase, for CuPc, the threshold voltage change also according to its value, without considering its direction.

	acid	acetone	IPAM	water	DMMP	H_2O_2	hexane	toluene
CuPc	red	light blue	red	orange	light blue	orange	orange	red
8-NTCDI	red	light blue	blue	orange	light blue	orange	orange	light blue
DMP-NTCDI	blue, blue	blue	blue	blue	orange	orange	light blue	red

Table 4. Sensor array qualitative mobility change map of different analytes. Blue spot represents large mobility decrease, two blue spots represent much large mobility decrease, while light blue spot means slight mobility decrease. The red spot represents a large mobility increase, two red spots represent a much larger mobility increase, and orange spot means a slight mobility increase.

	acid	acetone	IPAM	water	DMMP	H_2O_2	hexane	toluene
CuPc	● (blue)	● (blue)	● (blue)	● (light blue)	●● (blue, blue)	● (orange)	● (light blue)	● (blue)
8-NTCDI	●● (blue, blue)	● (red)	● (light blue)	● (blue)	● (red)	● (light blue)	● (light blue)	● (blue)
DMP-NTCDI	● (red)	● (blue)	● (light blue)	● (blue)	● (orange)	● (light blue)	● (light blue)	● (red)

and DMMP. This result is consisting with previous literature, reporting that CuPc is able to detect several ppm amine or ammonia.[2]

All these devices show excellent stable sensing behavior and excellent recovery ability. The recovery time can be markedly shortened by gently flowing dry nitrogen on the device surface or slightly warming the devices (about 35 °C to 40 °C) while applying the vacuum. As we discussed, for 8-NTCDI, on exposure to acetone and DMMP, there were initial current decreases due to the trapping effect of acetone and DMMP. During the recovery period, there was an initial current increase (the part between the blue and red arrows) on applying vacuum to remove analytes, the current then started to decease to its original value.

We also investigated the sensing behavior in several analyte mixtures (see Supporting Information, Figure S4–S6 and explanations included with them). For example, the dramatic DMP-NTCDI current-increase response to acetic acid was apparent even in the mixture with seven other analytes. 8-NTCDI could display the current increase from IPAm in mixtures including one with analytes that otherwise produce current decreases. Thus, the sensor array maintains analyte discrimination ability not only when exposed to single analyte vapors, but also in the presence of some analyte mixtures.

3. Conclusions

We have successfully discriminated as many as eight analytes (acetic acid, acetone, IPAm, DMMP, water, hydrogen peroxide, hexane and toluene) by a sensor array containing only three semiconductors. This sensor array gives different responses to all these analytes; the differences of responses (current, mobility and threshold voltage changes) are not only in the magnitude but also in the direction. The time evolutions of the responses are also different. These results demonstrate promise for such sensor arrays in analyte detection and discrimination. Furthermore, the responses of sensors in the array show excellent concentration dependence, and these devices exhibit excellent stable sensing behavior and recovery ability. Additionally,

the sensor array can even distinguish analytes from some complicated analyte mixtures. In particular, we project that the addition of a limited number of semiconductor molecules functionalized to influence mobility and threshold voltage in ways that are contrary to the usual rules of organic semiconductor design can add response diversity and response uniqueness for individual analytes to transistor sensor or chemiresistor arrays. To the best of our knowledge, this is one of the most efficient sensor arrays in terms of response pattern differentiation per number of devices based on OFETs with small organic molecules as semiconductor layers.

4. Experimental Section

All chemicals were purchased from Aldrich unless noted; N,N'-dioctyl naphthalenetetracarboxylic diimide (8-NTCDI) and dimethylpropylamine naphthalenetetracarboxylic diimide (DMP-NTCDI) were synthesized according to previous literature,[13] and purified by triple sublimations. Highly n-doped <100> silicon wafers with 300 nm of thermally grown oxide were diced into 1 in. by 1 in. substrates. The wafers were cleaned by sonication in acetone and isopropanol, and then dried in forced nitrogen gas. Substrates were dried more thoroughly via 100 °C vacuum annealing for 20 min prior to a 2-h exposure to hexamethyldisilazane (HMDS) vapor at 100 °C in a loosely sealed vessel. CuPc, 8-NTCDI and DMP-NTCDI were thermally evaporated onto HMDS treated substrates at room temperature with a thickness of 30 nm (10 nm for CuPc), and then gold electrodes were evaporated through a shadow mask (W = 8000 μm, L = 250 μm) to the thickness of 50 nm. All these OFETs were utilized in a vacuum probe station (Janis Research) with a calculated internal volume of 2.6 L attached to a Keithley 4200 semiconductor characterization system. All the analytes were injected by micro-syringe into the chamber and fully vaporized at high vacuum; here, the volume of all liquid analytes injected into the chamber is 10 μL except acetone (100 μL), hexane (40 μL) and toluene (30 μL) due to the low sensitivity of the OFET arrays to them. After converting to "ppm", the concentration is 1500 ppm for acetic acid, 11700 ppm for acetone, 1000 ppm for isopropylamine (IPAm), 4700 ppm for water, 800 ppm for dimethyl methylphosphonate (DMMP), 3800 ppm for hydrogen peroxide, 2600 ppm for hexane and 2400 ppm for toluene. Hydrogen peroxide exposure experiments were done as described in previous literature.[17] All data were acquired at 298K. The responses of these devices to analyte vapors were investigated by plotting the percent change in

www.MaterialsViews.com

ADVANCED
FUNCTIONAL
MATERIALS
www.afm-journal.de

FULL PAPER

Table 5. Numbers of trials and depositions leading to standard deviations presented in Figure 3–5.

	acetone	acid	IPAM	water	DMMP	H_2O_2	hexane	toluene
CuPc	3/3	3/3	6/3	4/3	3/3	3/3	3/3	3/3
8- NTCDI	7/5	3/3	5/5	5/3	4/4	3/3	3/3	3/3
DMP-NTCDI	7/5	5/5	4/3	7/5	6/5	4/3	3/3	3/3

Number of analyte exposure tests/number of different individual depositions of semiconductors.

drain current, $100\% \times (I_d - I_{d,0})/I_{d,0}$ (measured at $V_g = -100$ V, $V_{ds} = -100$ V for CuPc, and $V_g = +100$ V, $V_{ds} = +100$ V for 8-NTCDI and DMP-NTCDI) versus time of exposure to the analytes. All the exposure experiments were repeated at least three times, and devices were from at least three individual depositions; this information is summarized in (**Table 5**). X-ray diffraction scans were acquired in Bragg-Brentano (θ–2θ) geometry using a Philips X-pert pro X-ray diffraction system. Scan parameters were: step size 0.026°. 2 μm × 2 μm AFM topography images were observed by tapping mode using Molecular imaging PicoPlus.

The values of mobility and threshold voltage (V_{th}) were extracted according to the following equations:[20]

$$I_{ds, sat}^{1/2} = (W\mu_{sat}C_i/2L)^{1/2} (V_g - V_{th}) \tag{1}$$

Where $I_{ds, sat}$ is the saturated drain current, W and L are the width and length of the transistor, C_i is the gate capacitance, μ_{sat} is the mobility of the transistor; V_{th} is the threshold voltage of the transistor. In $I_{ds, sat}^{1/2}$–V_g curves, the cross point of the tangent of the curve with the x axis (V_g axis) at $I_d^{1/2}$ equal to zero is the value of threshold voltage, The mobility can be extracted from the slope of the tangent of $I_{ds, sat}^{1/2}$–V_g curve:

$$\text{Slope} = (W\mu_{sat}C_i/2L)^{1/2} \tag{2}$$

Supporting Information

Supporting Information is available from the Wiley Online Library or from the author.

Acknowledgements

[1] a) L. Torsi, A. Dodabalapur, L. Sabbatini, P. G. Zambonin, *Sens. Actuators B* **2000**, *67*, 312; b) B. Crone, A. Dodabalapur, A. Gelperin, L. Torsi, H. E. Katz, A.J. Lovinger, Z. Bao, *Appl. Phys. Lett.* **2001**, *78*, 2229; c) K. C. See, A. Becknell, J. Miragliotta, H. E. Katz, *Adv. Mater.* **2007**, *19*, 3322; d) K. Potje-Kamloth, *Chem. Rev.* **2008**, *108*, 367; e) J. Huang, T. J. Dawidczyk, B. J. Jung, J. Sun, A. F. Mason, H. E. Katz, *J. Mater. Chem.* **2010**, *20*, 2644; f) T. Someya, A. Dodabalapur, J. Huang, K. C. See, H. E. Katz, *Adv. Mater.* **2010**, *22*, 3799; g) J. Huang, J. Sun, H. E. Katz, *Adv. Mater.* **2008**, *20*, 2567; h) J. Huang, J. Miragliotta, A. Becknell, H. E. Katz, *J. Am. Chem. Soc.* **2007**, *129*, 9366; i) M. L. Hammock, A. N. Sokolov, R. M. Stoltenberg, B. D. Naab, Z. N. Bao, *ACS Nano* **2012**, *6*, 3100; j) L. Torsi, G. M. Farinala, F. Marinelli, M. C. Tanese, O. H. Omar, L. Valli, F. Babudri, F. Palmisano, P. G. Zambonin, F. Naso, *Nat. Mater.* **2008**, *7*, 412; k) C. Kim, Z. M. Wang, H-J. Choi, Y-G. Ha, A. Facchetti, T. J. Marks, *J. Am. Chem. Soc.* **2008**, *130*, 6867; l) A. N. Sokolov, B. C-K. Tee, C. J. Bettinger, J. B.-H. Tok, Z. N. Bao, *Acc. Chem. Res.* **2012**, *45*, 361; m) J. E. Royer, C. Y. Zhang, A. C. kummel, W. C. Trogler, *Langmuir* **2012**, *28*, 6192; n) F. I. Bohrer, C. N. Colesniuc, J. Park, M. E. Ruidiaz, I. K. Schuller, A. C. Kummel, W. C. Trogler, *J. Am. Chem. Soc.* **2009**, *131*, 478; o) F. I. Bohrer, A. Sharoni, C. N. Colesniuc, J. Park, I. K. Schuller, A. C. Kummel, W. C. Trogler, *J. Am. Chem. Soc.* **2007**, *129*, 5640; p) M. C. Mcalpine, H. Ahmad, D. Wang, J. R. Heath, *Nat. Mater.* **2007**, *6*, 379.

[2] a) W.G. Huang, K. Besar, R. LeCover, A. M. Rule, P. N. Breysse, H. E. Katz, *J. Am. Chem. Soc.* **2012**, *134*, 14650; b) M. Bouvet, H. Xiong, V. Parra, *Sens. Actuators B* **2010**, *146*, 501; c) Y. L. Chen, M. Bouvet, T. Sizun, G. Barochi, J. Rossignol, E. Lesniewska, *Sens. Actuators B* **2011**, *155*, 165; d) H.-W. Zan, C.-H. Li, C.-C. Yeh, M.-Z. Dai, H.-F. Meng, C.-C. Tsai, *Appl. Phys. Lett.* **2011**, *98*, 253503; e) B. Esser, J. M. Schnorr, T. M. Swager, *Angew. Chem. Int. Ed.* **2012**, *51*, 5752; f) A. Das, R. Dost, T. Richardson, M. Grell, J. J. Morrison, M. L. Turner, *Adv. Mater.* **2007**, *19*, 4018.

[3] a) H. Kong, B. J. Jung, J. Sinha, H. E. Katz, *Chem. Mater.* **2012**, *24*, 2621; 3 b) H. Kong, J. Sinha, J. Sun, H. E. Katz, *Adv. Funct. Mater.* **2013**, *23*, 91.

[4] a) H. U. Khan, M. E. Roberts, W. Knoll, Z. N. Bao, *Chem. Mater.* **2011**, *23*, 1946; b) M. E. Roberts, M. C. LeMieux, Z. N. Bao, *ACS Nano* **2009**, *3*, 3287; c) A. N. Sokolov, M. E. Johnson, O. B. Roberts, Y. Cao, Z. N. Bao, *Adv. Mater.* **2010**, *22*, 2349; d) G. Gruner, *Anal Bioanal Chem.* **2006**, *384*, 322; e) T.-W. Lin, P.-J. Hsieh, C.-L. Lin, Y.-Y. Fang, J.-X. Yang, C.-C. Tsai, P.-L. Chiang, C.-Y. Pan, Y.-T. Chen, *Proc. Natl. Acad. Sci. USA* **2010**, *107*, 1047; f) M. D. Angione, S. Cotrone, M. Magliulo, A. Mallardi, D. Altamura, C. Giannini, N. Cioffi, L. Sabbatini, E. Fratini, P. Baglioni, G. Scamarcio, G. Palazzo, L. Torsi, *Proc. Natl. Acad. Sci. USA* **2012**, *109*, 6429; g) Z-T. Zhu, J. T. Mabeck, C. Zhu, N. C. Cady, C. A. Batt, G. G. Malliaras, *Chem. Commun.* **2004**, 1556.

[5] a) F. Liao, S. Yin, M. F. Toney, V. Subramanian, *Sens. Actuators B* **2010**, *150*, 254; b) M. Castro, B. Kumar, J. F. Feller, Z. Haddi, A. Amari, B. Bouchikhi, *Sens. Actuators B* **2011**, *159*, 213; c) J. Cai, C. Yao, J. Xia, J. Wang, M. Chen, J. Huang, K. Chang, C. Liu, H. Pan, W. Fu, *Sens. Actuators B* **2011**, *155*, 500; d) B. P. Regmi, J. Monk, B. EI-Zahab, S. Das, F. R. Hung, D. J. Hayes, I. M. Warner, *J. Mater. Chem.* **2012**, *22*, 13732; e) A. Rehman, A. Hamilton, A. Chung, G. A. Baker, Z. Wang, X. Zeng, *Anal. Chem.* **2011**, *83*, 7823; f) D. Croux, A. Weustenraed, P. Pobedinska, F. Horemans, H. Dilien, K. Haenen, T. Cleij, P. Wagner, R. Thoelen, W. D. Ceuninck, *Phys. Status Solidi A* **2012**, *209*, 892; g) C.-L. Li, Y.-F. Chen, M.-H. Liu,

FULL PAPER

C.-J. Lu, *Sens. Actuators B* **2012**, *169*, 349; h) D. D. Erbahar, I. Gürol, G. Gümüs, E. Musluoglu, Z. Z. öztürk, V. Ahsen, M. Harbeck, *Sens. Actuators B* **2012**, *173*, 562; i) P. Resa, P. Castro, J. Rodrigues-Lopez, L. Elvira, *Sens. Actuators B* **2012**, *166-167*, 275; j) X. Fan, B. Du, *Sens. Actuators B* **2011**, *160*, 724; k) J. Tang, E. Skotadis, S. Stathopoulos, V. Roussi, V. Tsouti, D. Tsoukalas, *Sens. Actuators B* **2012**, *170*, 129; l) D. C. Wedge, A. Das, R. Dost, J. Kettle, M.-B. Madec, J. J. Morrison, M. Grell, D. B. Kell, T. H. Richardson, S. Yeates, M. L. Turner, *Sens. Actuators B* **2009**, *143*, 365; m) B. A. Suslick, L. Feng, K. S. Suslick, *Anal. Chem.* **2010**, *82*, 2067.

[6] B. Li, G. Sauvé, M. C. Iovu, M. Jeffeies-EL, R. Zhang, J. Cooper, S. Santhanam, L. Schultz, J. C. Revelli, A. G. Kusne, T. Kowalewski, J. L. Snyder, L. E. Weiss, G. K. Fedder, R. D. McCullough, D. N. Lambeth, *Nano Lett* **2006**, *6*, 1598.

[7] F. Wang, T. M. Swager, *J. Am. Chem. Soc.* **2011**, *133*, 11181.

[8] J. A. Covington, J. W. Gardner, P. N. Bartlett, C-S. Toh, *IEEE Proc.-Circuits Devices Syst.* **2004**, *151*, 326.

[9] M. D. Shirsat, T. Sarkar, J. K. N. V. Myung Jr., B. Konnanath, A. Spanias, A. Mulchandani, *J. Phys. Chem. C* **2012**, *116*, 3845.

[10] M. Bora, D. Schut, M. A. Baldo, *Anal. Chem.* **2007**, *79*, 3298.

[11] U. Lange, N. V. Roznyatovskaya, V. M. Mirsky, *Anal. Chim. Acta* **2008**, *614*, 1.

[12] H. Lin, M. Jang, K. S. Suslick, *J. Am. Chem. Soc.* **2011**, *133*, 16786.

[13] H. E. Katz, A. J. Lovinger, J. Johnson, C. Kloc, T. Siegrist, W. Li, Y. Y. Lin, A. Dodabalapur, *Nature* **2000**, *404*, 478.

[14] H. Graaf, D. Schlettwein, *J. Appl. Phys.* **2006**, *100*, 126104.

[15] a) D. Duarte, A. Dodabalapur, *J. Appl. Phys.* **2012**, *111*, 044509; b) *The Phthalocyanines* Vol.*1–4* (Ed.: C. C. Leznoff, A. B. P. Lever), Wiley, New York 1986–1993; c) *Phthalocyanine Materials-Synthesis, Structure and Function*, (Ed: N. B. McKeown), Cambridge University Press, Cambridge, UK **1998**; d) Y. Chen, W. G. Huang, C. H. Li, Z. S. Bo, *Macromolecules* **2010**, *43*, 10216.

[16] N. J. Tremblay, B. J. Jung, P. Breysse, H. E. Katz, *Adv. Funct. Mater.* **2011**, *21*, 4314.

[17] a) F. I. Bohrer, C. N. Colesniuc, J. Park, I. K. Schuller, A. C. Kummel, W. C. Trogler, *J. Am. Chem. Soc.* **2008**, *130*, 3712; b) G. Mastrangelo, R. Zanibellato, E. Fadda, J. H. Lange, L. Scoizzato, R. Rylander, *Ann. Occup. Hyg.* **2009**, *53*, 161.

[18] T. Jung, A. Dodabalapur, *Appl. Phys. Lett.* **2005**, *87*, 182109.

[19] B. Li, S. Santhanam, L. Schultz, M. Jeffeies-EL, M. C. Iovu, G. Sauvé, J. Cooper, R. Zhang, J. C. Revelli, A. G. Kusne, J. L. Snyder, T. Kowalewski, L. E. Weiss, R. D. McCullough, G. K. Fedder, D. N. Lambeth, *Sens. Actuators B* **2007**, *123*, 651.

[20] J. Zaumseil, H. Sirringhaus, *Chem. Rev.* **2007**, *107*, 1296.